

Viscoelasticity and surface tension at the defect-induced first-order melting transition of a vortex lattice

Hervé M. Carruzzo and Clare C. Yu

Department of Physics and Astronomy, University of California, Irvine, Irvine, California 92697

(Received 2 August 1999)

We show that thermally activated interstitial and vacancy defects can lead to first-order melting of a vortex lattice. We obtain good agreement with experimentally measured melting curve, latent heat, and magnetization jumps for $\text{YBa}_2\text{Cu}_3\text{O}_{7-\delta}$ and $\text{Bi}_2\text{Sr}_2\text{CaCu}_2\text{O}_8$. The shear modulus of the vortex liquid is frequency dependent and crosses over from zero at low frequencies to a finite value at high frequencies. We also find a small surface tension between the vortex line liquid and the vortex lattice.

I. INTRODUCTION

It has been experimentally established that below a critical value of the magnetic field, vortex lattices undergo a first-order transition in clean high-temperature superconductors.¹⁻⁴ This has been seen in $\text{YBa}_2\text{Cu}_3\text{O}_{7-\delta}$ (YBCO),⁵⁻¹¹ $\text{Bi}_2\text{Sr}_2\text{CaCu}_2\text{O}_8$ (BSCCO),¹²⁻¹⁴ and $(\text{La}_{1-x}\text{Sr}_x)_2\text{CuO}_4$.¹⁵ Evidence for first-order phase transitions comes from latent heat measurements⁸ and peaks in the specific heat^{16,9,11} as well as jumps in the resistivity^{5,13,14} and in the magnetization.^{17,6,7,12,15} This transition is generally accepted as a melting transition from a vortex solid to a vortex liquid.

A great deal of theoretical work¹⁸⁻²⁸ has helped to establish that there is a first-order melting transition. Brézin, Nelson, and Thiaville¹⁸ showed that including fluctuation effects in Abrikosov's mean-field theory of the flux lattice transition would drive the transition first-order. The advent of the high-temperature superconductors and the subsequent experimental indications of vortex lattice melting sparked intense theoretical activity. Early analytic efforts used the Lindemann criterion,¹⁹ though such an approach could not show that the transition was first order. Studies of the mapping between vortex lines and the world lines of a two-dimensional (2D) system of bosons have suggested a first-order transition from an Abrikosov lattice to an entangled vortex liquid.^{1,29,28} Numerical simulations^{20-27,30} have been able to show that the melting is first order by calculating quantities such as the magnetization jump^{21,23} and the delta function in the specific heat.^{24,25,27} However these simulations were done in the limit of high magnetic fields $\xi_{ab} \ll a_0 \ll \lambda_{ab}$ where ξ_{ab} is the coherence length, a_0 is the spacing between vortices, and λ_{ab} is the penetration depth. Most^{20,21,23-27} assumed that the magnetic induction \mathbf{B} was spatially uniform and thus neglected the wave-vector dependence of the elastic moduli. This has made quantitative comparison with experimental data difficult, especially in the case of BSCCO whose vortex lattice melts at low fields. In addition the mechanism for vortex lattice melting is still not well established. There have been suggestions that topological defects³¹ such as vortex loops,^{26,27} vortex-antivortex pairs,^{24,25} free disclinations,²² and dislocations³² may play a key role in triggering melting.

Melting scenario

In this paper we show that melting can be induced by interstitial and vacancy line defects in the vortex lattice which soften the shear modulus c_{66} . This softening makes it easier to introduce more defects and increases the vibrational free energy. The increased vibrations ultimately lead to melting. There is good agreement with the experimental curve of transition temperature versus field, latent heat, and magnetization jumps for YBCO and BSCCO. Using a viscoelastic approach, we show that the shear modulus is frequency dependent. At zero frequency the vortex liquid cannot sustain a shear while at high frequency the liquid has a finite shear modulus. Since we can calculate the free energy for both the lattice and the liquid at melting, we have estimated the surface tension between a vortex line liquid and a vortex solid.

Let us describe our scenario for melting. Our approach follows that of Granato³³ as well as previous work which showed that defects can lead to a first-order phase transition.³⁴ We start with a vortex lattice in a clean layered superconductor with a magnetic field H applied perpendicular to the layers along the c axis. We consider the vortices to be correlated stacks of pancake vortices. We will assume that the transition is induced by topological defect lines, i.e., vacancies and interstitials. In a Delaunay triangulation³⁵ a vacancy or an interstitial in a triangular lattice is topologically equivalent to a pair of bound dislocations²² as well as to a twisted bond defect.³⁶ High-temperature decoration experiments³⁶ and Monte Carlo simulations²² have found such defects to be thermally excited. The introduction of these defects softens the elastic moduli. Since the energy to introduce interstitials and vacancies is proportional to the elastic moduli, softening makes it easier to introduce more defects. The softening also increases the vibrational entropy of the vortex lattice which leads to a melting transition. *The transition is driven by the increased vibrational entropy of the ordinary vortex lines of the lattice, and not by the entropy of the wandering of the defect lines.* In fact Frey, Nelson, and Fisher³⁷ showed that a phase transition driven by the entropy of wandering flux lines occurs at a much higher magnetic field than what is observed experimentally. In the vicinity of the experimentally observed first-order phase transition, wandering in the transverse direction by more than a lattice spacing is energetically quite costly and there-

fore rare. Such flux line bending also makes dislocations^{38,39} energetically costly at low dislocation densities. [The energy scale is set by $\epsilon_0 s$.^{3,4} Here s is the interplane spacing and ϵ_0 , the energy per unit length of a vortex, is given by $\epsilon_0 = (\phi_0/4\pi\lambda_{ab})^2$ where ϕ_0 is the flux quantum and λ_{ab} is the penetration depth for currents in the ab plane. For example, for YBCO $\epsilon_0 s \sim 650$ K at $T=70$ K and for BSCCO $\epsilon_0 s \sim 550$ K at $T=60$ K.⁴⁰ Note that $\epsilon_0 s \gg T$.]

The first-order transition is nucleated in a small region by a local rearrangement of existing line segments. Slightly above the melting temperature T_m a vortex line can distort and make an interstitial and a vacancy line segment that locally melt the solid. This is the analog of a liquid droplet which nucleates melting of a crystal. The role of the surface tension is played by the energy to connect the interstitial segment to the rest of the vortex line. This connection can be a Josephson vortex lying between planes or a series of small pancake vortex displacements spread over several layers. When the length l of the interstitial and vacancy segments equals the critical length l_c , the energy gained by melting equals the energy cost of the connections. When $l > l_c$, it is energetically favorable for the defect segments to grow to the length of the system. We are ignoring the surface tension associated with the surface parallel to the c axis. We shall show later that this is quite small.

II. FREE ENERGY

To study melting we assume that we have a vortex lattice with interstitial and vacancy lines extending the length of the lattice. Our goal is to find the free-energy density as a function of the concentration n of defect lines. The free-energy density is

$$f = f_0 + f_w + f_{vib} + f_{wan}, \quad (1)$$

where f_0 is the free-energy density of a perfect lattice, f_w is the work needed to introduce a straight interstitial or vacancy line into the lattice, f_{vib} is the vibrational free energy density of the system, and f_{wan} is the free-energy due to the wandering of the defect lines over distances large compared to the lattice spacing. We now examine these terms in detail.

f_0 , the free-energy density of a perfect rigid flux lattice, is given by the London term:^{37,41}

$$f_0 = \frac{B^2}{8\pi} + \frac{B\phi_0}{32\pi^2\lambda_{ab}^2} \ln\left(\frac{\eta\phi_0}{2\pi\xi_{ab}^2 B}\right), \quad \frac{\phi_0}{4\pi\lambda_{ab}^2} \ll B \ll H_{c2}, \quad (2)$$

where B is the spatially averaged magnetic induction, ξ_{ab} is the coherence length in the ab plane, and η is 0.130 519 for a hexagonal lattice and 0.133 311 for a square lattice.³⁷ For B near H_{c2} , f_0 is given by the Abrikosov free-energy⁴²

$$f_0 = \frac{B^2}{8\pi} - \frac{(H_{c2} - B)^2}{8\pi[1 + (2\kappa^2 - 1)\beta_A]}, \quad (3)$$

where the Ginzburg-Landau parameter $\kappa = \lambda_{ab}/\xi_{ab}$, and the Abrikosov parameter β_A is 1.16 for a triangular lattice and 1.18 for a square lattice.

To calculate f_{vib} , we follow Ref. 43. We denote the displacement of the ν th vortex pancake in the n th plane from its

equilibrium position by $\mathbf{u}(n, \mathbf{r}_\nu)$ where $\mathbf{u} = (u_x, u_y)$ and the pancake position $\mathbf{r} = (r_x, r_y)$. The Fourier transform $\mathbf{u}(\mathbf{k}, q) = \sum_{n\nu} \mathbf{u}(n, \mathbf{r}_\nu) \exp[i(\mathbf{k} \cdot \mathbf{r}_\nu + qn)]$. $\mathbf{k} = (k_x, k_y)$ and q is the wave vector along the c axis.

$$f_{vib} = -(k_B T/V) \ln Z_{vib}, \quad (4)$$

where V is the volume and the vibrational partition function Z_{vib} is given by

$$Z_{vib} = \int e^{-\mathcal{F}_{el}/k_B T} \prod_{\mathbf{k}, q > 0, i} \frac{du_R(i\mathbf{k}, q) du_I(i\mathbf{k}, q)}{\pi \xi_{ab}^2}, \quad (5)$$

where we have divided by the area $\pi \xi_{ab}^2$ of the normal core of a pancake.⁴³ u_R and u_I are the real and imaginary parts of $\mathbf{u}(\mathbf{k}, q)$ and $i \in \{x, y\}$. The elastic free-energy functional associated with these distortions is

$$\mathcal{F}_{el} = \frac{1}{2} v_0 \sum_{\mathbf{k}q} \sum_{ij} u_i(\mathbf{k}, q) a_{ij} u_j^*(\mathbf{k}, q), \quad (6)$$

where i and $j \in \{x, y\}$, the volume per pancake vortex is $v_0 = s\phi_0/B$, and s is the interplane spacing. The \mathbf{k} sum is over a circular Brillouin zone $K_0^2 = 4\pi B/\phi_0$. The matrix a_{ij} is given by

$$a_{ij} = c_B k_i k_j + (c_{66} k^2 + c_{44} Q^2) \delta_{ij}, \quad (7)$$

where c_B , c_{66} , and c_{44} are the bulk, shear, and tilt moduli, respectively. $c_B = c_{11} - c_{66}$ for a hexagonal lattice. $Q^2 = 2(1 - \cos qs)/s^2$. Diagonalizing a_{ij} leads to two eigenvalues:

$$A_l(kq) = c_{11} k^2 + c_{44} Q^2, \\ A_t(kq) = c_{66} k^2 + c_{44} Q^2, \quad (8)$$

where A is the diagonal matrix, the subscript l denotes longitudinal, and t denotes transverse. Using this leads to

$$\mathcal{F}_{el} = \frac{1}{2} v_0 \sum_{\mathbf{k}q} \sum_{i=l,t} A_i |u_i(\mathbf{k}, q)|^2, \quad (9)$$

where $i \in \{l, t\}$. After integrating over u in Eq. (5), the remaining sums over \mathbf{k} and q are converted to integrals:

$$\ln Z_{vib} = \sum_{i=l,t} \frac{1}{2} \int_0^{K_0^2} \frac{d(k^2)}{4\pi} \int_{-\pi/s}^{\pi/s} \frac{dq}{2\pi} \ln \left(\frac{2k_B T}{v_0 \xi_{ab}^2 A_i} \right), \quad (10)$$

where the volume of the sample is set to unity. The integrals in Eq. (10) are done numerically. At low fields ($b = B/H_{c2} < 0.25$), the elastic moduli are given by^{3,4,44}

$$c_{66} = \frac{B\phi_0 \zeta}{(8\pi\lambda_{ab})^2},$$

$$c_{11} = \frac{B^2 [1 + \lambda_c^2 (k^2 + Q^2)]}{4\pi [1 + \lambda_{ab}^2 (k^2 + Q^2)] (1 + \lambda_c^2 k^2 + \lambda_{ab}^2 Q^2)},$$

$$c_{44} = \frac{B^2}{4\pi(1+\lambda_c^2 k^2 + \lambda_{ab}^2 Q^2)} + \frac{B\phi_0}{32\pi^2\lambda_c^2} \ln \frac{\xi_{ab}^{-2}}{K_0^2 + (Q/\gamma)^2 + \lambda_c^{-2}} + \frac{B\phi_0}{32\pi^2\lambda_{ab}^4 Q^2} \ln \left(1 + \frac{Q^2}{K_0^2} \right) \quad (11)$$

where λ_c is the penetration depth for currents along the c axis, $\gamma = \lambda_c/\lambda_{ab}$ is the anisotropy, and $\zeta = 1$. At high fields ($b > 0.5$),^{3,4,45} c_{66} is altered by the factor $\zeta \approx (1 - 0.5\kappa^{-2})(1-b)^2(1-0.58b+0.29b^2)$ and the penetration depths in c_{11} and c_{44} are replaced by $\tilde{\lambda}^2 = \lambda^2/(1-b)$ where λ denotes either λ_{ab} or λ_c . In addition the last two terms of c_{44} are replaced by $B\phi_0/(16\pi^2\tilde{\lambda}_c^2)$. These replacements guarantee that the elastic moduli vanish at H_{c2} . For YBCO the temperature dependence of the penetration depths and coherence lengths are given by $\lambda(T) = \lambda(0)[1 - (T/T_c)]^{-1/3}$ (Ref. 46) and $\xi_{ab}(T) = \xi_{ab}(0)[1 - (T/T_c)]^{-1/2}$, respectively. For BSCCO whose melting field is two orders of magnitude below H_{c2} , $\lambda^2(T) = \lambda^2(0)/[1 - (T/T_c)^4]$ and $\xi_{ab}^2(T) = \xi_{ab}^2(0)/[1 - (T/T_c)^4]$.⁴¹

The free-energy density f_w due to the energy cost of adding a vacancy or interstitial vortex line is difficult to calculate accurately.^{37,47} However, we can write down a plausible form for f_w by noting that a straight-line defect parallel to the c axis produces both shear and bulk (but not tilt) distortions of the vortex lattice. For example, if a defect at the origin produces a displacement \mathbf{u} that satisfies $\nabla \cdot \mathbf{u} = \nu_0 \delta(\mathbf{r})/s$ where $\delta(\mathbf{r})$ is a two-dimensional delta function, then $u_\alpha(\mathbf{k}) = ik_\alpha/k^2$.^{37,48} Inserting this in Eq. (6), we find that $f_w = (c_{66} + \bar{c}_B)/2$ where $\bar{c}_B = \sum_{\mathbf{k}} c_B(q=0, \mathbf{k})$. Generalizing this to allow for a more complicated distortion and for a concentration n of line defects, we write³³

$$f_w = \int_0^n dn (\alpha_1 c_{66} + \alpha_2 \bar{c}_B), \quad (12)$$

where α_1 and α_2 are dimensionless constants. We expect the isotropic distortion to be small, i.e., $\alpha_2 \ll 1$, and the shear deformation to dominate, i.e., $\alpha_1 \gg \alpha_2$. Integrating over n allows the elastic moduli to depend on defect concentration. We will assume that c_B is independent of n since we believe that the bulk modulus of the vortex solid is roughly the same as that of the liquid phase. To find $c_{66}(n)$,³³ we use its definition

$$c_{66} = \partial^2 f / \partial \varepsilon^2, \quad (13)$$

where ε is the shear strain. Assuming that c_B has negligible shear strain dependence, we find

$$c_{66}(n) = c_{66}(0) + \alpha_1 \int_0^n [\partial^2 c_{66}(n) / \partial \varepsilon^2] dn \quad (14)$$

or

$$\frac{\partial c_{66}(n)}{\partial n} = \alpha_1 \frac{\partial^2 c_{66}(n)}{\partial \varepsilon^2}. \quad (15)$$

If we shear the lattice in the ab plane along rows separated by a distance d , the system must be unchanged if the displacement is equal to a lattice spacing. This is a result of the

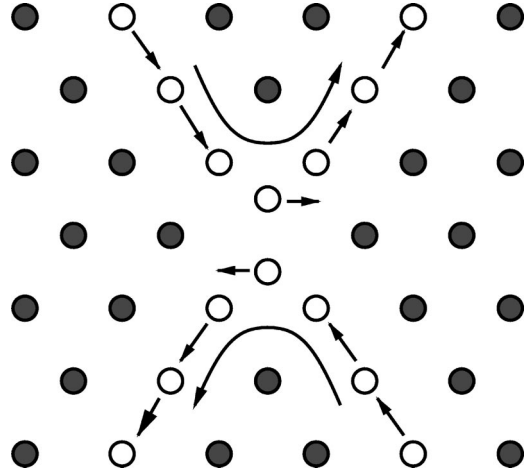


FIG. 1. Dumbbell interstitial configuration in a triangular lattice introduces a stringlike librational resonance mode that couples to external shear stress and softens the shear modulus. The atoms or flux lines involved in this mode are shown with open circles while the rest of the sites are denoted by solid circles.

discrete translational symmetry of the lattice. The shear modulus should reflect this discrete translational symmetry and therefore must be periodic in displacements equal to the lattice constant $a_0 = \sqrt{\phi_0}/B$. We describe this with the simplest even periodic function:

$$c_{66}(u) = c_{66}(u=0) \cos(2\pi u/a_0), \\ = c_{66}(\varepsilon=0) \cos(2\pi d\varepsilon/a_0), \quad (16)$$

where the shear strain $\varepsilon = u/d$. Notice that this expression goes beyond the usual harmonic approximation. Then taking the second derivative of Eq. (16) we obtain

$$\partial^2 c_{66}(n) / \partial \varepsilon^2 = -\beta c_{66}(n), \quad (17)$$

where $\beta = 4\pi^2 d^2/a_0^2$. Combining this with Eq. (15), we obtain

$$c_{66}(n) = c_{66}(0) \exp(-\alpha_1 \beta n), \quad (18)$$

where $c_{66}(0)$ is given in Eq. (11). Thus the shear modulus softens exponentially with the defect concentration n . This softening lowers the energy cost to introduce further defects, and increases the vibrational free energy f_{vib} when $c_{66}(n)$ is used in a_{ij} . Substituting $c_{66}(n)$ in Eq. (18) into our expression (12) for f_w yields

$$f_w = \frac{c_{66}(n=0)}{\beta} (1 - e^{-\alpha_1 \beta n}) + \alpha_2 \bar{c}_B n. \quad (19)$$

The softening of the shear modulus with increasing defect concentration is well known in the case of atomic lattices.⁴⁹ There it has been shown both experimentally⁵⁰⁻⁵² and theoretically⁵³ that interstitials can substantially soften the elastic constants with the largest change being in the shear modulus. Linear extrapolation of the experimentally measured change of the shear modulus of copper would imply that the lattice becomes unstable for a concentration of about 3% interstitials.⁴⁹ An example of how interstitials can soften the shear modulus is illustrated in Fig. 1. Here we show a

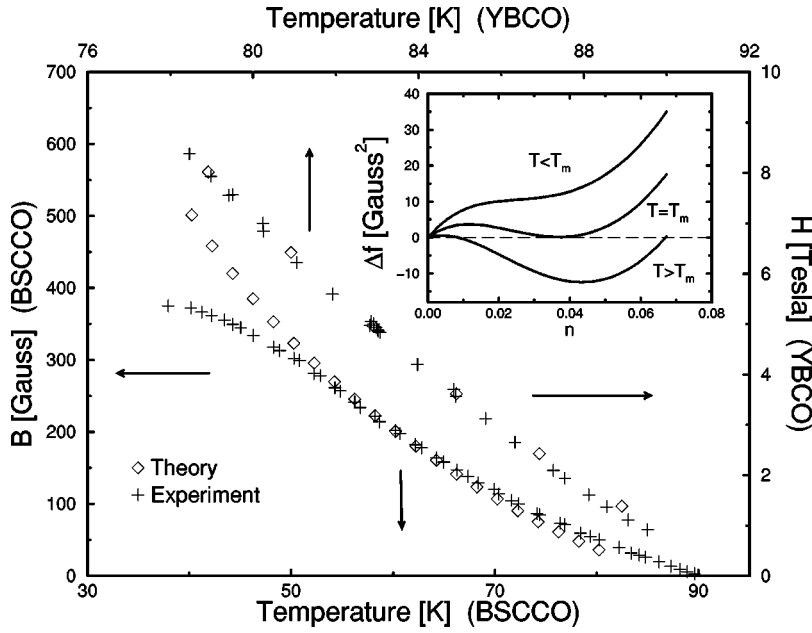


FIG. 2. First-order phase transition curves of magnetic field versus temperature for YBCO and BSCCO. Parameters used for YBCO are $\alpha_1 = 2.55$, $\alpha_2 = 0.01485$, $\phi = 44.1^\circ$, $\lambda_{ab}(0) = 1186 \text{ \AA}$ (Ref. 46), $s = 12 \text{ \AA}$, $\xi_{ab}(0) = 15 \text{ \AA}$, $\gamma = 5$, and $T_c = 92.74 \text{ K}$. Parameters used for BSCCO are $\alpha_1 = 1.0$, $\alpha_2 = 0.00705$, $\phi = 60^\circ$, $\lambda_{ab}(0) = 2000 \text{ \AA}$, $s = 14 \text{ \AA}$, $\xi_{ab}(0) = 30 \text{ \AA}$, $\gamma = 200$, and $T_c = 90 \text{ K}$. For BSCCO we use the low field form of the elastic moduli from Eq. (11) and for YBCO we use the high-field form. For f_0 we use Eq. (2) for BSCCO and Eq. (3) for YBCO. (For BSCCO we plot B vs T because that is what Ref. 12 measured). The experimental points for YBCO come from Ref. 8 and those for BSCCO come from Ref. 12. Inset: Typical Δf versus n .

triangular lattice where an interstitial forms a dumbbell aligned in the $\langle 010 \rangle$ direction by sharing a site with another atom or flux line. Dumbbell displacements along the $\langle 100 \rangle$ direction introduce a stringlike librational resonance mode consisting of displacements along the $\langle 110 \rangle$ directions. This mode couples strongly to an external shear stress and results in softening of the shear modulus.⁵⁴

The last term we need to consider is f_{wan} , the free energy due to the wandering of the defect lines over distances large compared to the lattice spacing. We can estimate f_{wan} with the following expression:³⁷

$$f_{wan} \approx -\frac{k_B T}{l_z a_0^2} \ln(m_l), \quad (20)$$

where $m_l = 3$ for a triangular lattice (BSCCO) and $m_l = 4$ for a square lattice (YBCO). l_z can be thought of as the distance along the z axis that it takes⁵⁵ for the defect line to wander a transverse distance of one lattice spacing a_0 . To go from one vacancy or interstitial site to the next, the defect line segment must jump over the barrier between the two positions. This gives l_z a thermally activated form: $l_z \sim l_0 \exp(E/k_B T)$, where $l_0 \approx a_0(\epsilon_1/\epsilon_B)^{1/2}$ and $E \approx a_0(\epsilon_1 \epsilon_B)^{1/2}$. ϵ_1 is the line tension and is given by $\epsilon_1 \sim (\epsilon_0/\gamma^2) \ln(a_0/\xi_{ab})$. Numerical simulations^{37,47} indicate that the barrier height ϵ_B is small and we use $\epsilon_B = 2.5 \times 10^{-3} \epsilon_0$. f_{wan} itself is quite small compared to the other terms because of the high-energy cost of vortex displacements. For example, at the transition f_{wan} is about two orders of magnitude smaller than f_w or f_{vib} . Thus the transition is not driven by a proliferation of wandering defect lines because near the transition the high-energy cost of vortex displacements is not sufficiently offset by the entropy of the meandering line.³⁷

Before we plot f versus n , we note that the difference between B and H is negligible for YBCO but can be a significant fraction of the melting field H_m for BSCCO. To find the value of B to use in the Helmholtz free-energy density f , we minimize the Gibbs free-energy density G , i.e., $\partial G/\partial B = 0$ where $G = f - \mathbf{B} \cdot \mathbf{H}/4\pi$. We find B for $n=0$ for each

value of H and T . Since the concentration dependence of B is negligible, the change in the Gibbs free energy due to the presence of defect lines is given by

$$\Delta G(H, n) = G(H, n) - G(H, n=0) = \Delta f(B(H), n), \quad (21)$$

where Δf is given by

$$\Delta f = f(n) - f(0) = f_w + \Delta f_{vib} + f_{wan}. \quad (22)$$

Typical plots of Δf versus n are shown in the inset of Fig. 2. The rise in Δf at large n is due to the compressional energy cost associated bulk modulus term in Eq. (19). The double-well structure of Δf is characteristic of a first-order phase transition. The equilibrium transition occurs when both minima have the same value of Δf . We associate the minimum at $n=0$ with the vortex solid and the minimum at finite n with the vortex liquid. The defect concentration at the transition is only a few percent. Equation (18) implies that a finite value of n yields a finite value for the shear modulus, e.g., for $n=5\%$, $c_{66}(n) \sim 0.2c_{66}(0)$ for BSCCO. Previous work³⁴ interpreted this to mean that the lattice did not melt. However, they did not appreciate the fact that the shear modulus is frequency dependent and the c_{66} used here is the high-frequency response. At high frequencies it is the elastic response which dominates and this is what enters into the expression for the free energy. For a liquid the low-frequency response is dominated by viscosity so that the zero-frequency shear modulus is zero. We will elaborate more on this later.

III. FITS TO EXPERIMENTAL DATA

A. Melting curve

In Fig. 2 we fit the experimental first-order transition curves in the H - T plane by plotting ΔG from Eq. (21) versus n for a given temperature and determining the field H where both minima have the same value of ΔG . We use two adjustable parameters α_1 and α_2 which are the proportionality constants between the free energy f_w to introduce a defect

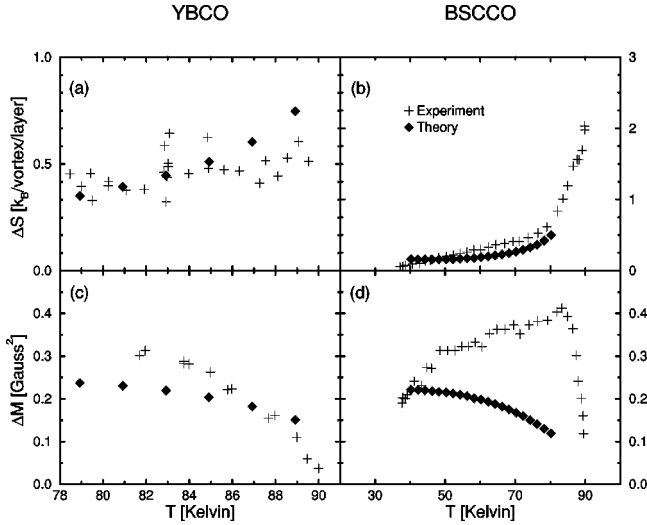


FIG. 3. (a) and (b): Entropy jump Δs per vortex per layer versus T_m at the transition for YBCO and BSCCO. The experimental points for YBCO are from Ref. 8 and those for BSCCO are from Ref. 12. (c) and (d): Magnetization jump ΔM versus T_m at the first-order phase transition for YBCO and BSCCO. The experimental points for YBCO are from Ref. 7 and those for BSCCO are from Ref. 12. For the theoretical points the values of the parameters are the same as in Fig. 1 for all the curves.

line and the elastic moduli. As expected, $\alpha_1 \gg \alpha_2$ and $\alpha_2 \ll 1$ (see Fig. 2). The geometrical quantity β can have several values for a given lattice structure, depending on which planes are sheared. We choose $\beta = \pi^2 \tan^2 \phi$ where ϕ is the angle between primitive vectors. Decoration experiments on BSCCO find a triangular lattice,³⁶ so we use $\phi = 60^\circ$. For YBCO we choose $\phi = 44.1^\circ$ which is very close to a square lattice which has $\phi = 45^\circ$. Maki⁵⁶ has argued that the d -wave symmetry of the order parameter yields a square vortex lattice tilted by 45° from the a axis. Experiments^{57–60} on YBCO find ϕ ranging from 36° to 45° .

B. Magnetization and entropy jumps

We can calculate the jump in magnetization ΔM at the transition using $\Delta M = -\partial \Delta G / \partial H|_{T=T_m}$ where $\Delta G = G(n_l) - G(n=0)$. Here n_l is the defect concentration in the liquid at the melting transition. The jump in entropy Δs is given by $\Delta s = -v_0 \partial \Delta G / \partial T|_{H=H_m}$ where Δs is the entropy change per vortex per layer. The results are shown in Fig. 3. We have checked that our results satisfy the Clausius-Clapeyron equation $\Delta s = -(v_0 \Delta B / 4\pi) dH_m / dT$. We obtain good agreement with experiment for YBCO and the right order of magnitude for BSCCO. The difference between theory and experiment in the temperature dependence of the entropy and magnetization jumps for BSCCO may be due to the decoupling of the planes.^{61–65} This enhances the thermal excursions and hence the entropy of the pancake vortices.^{66–68} Decoupling may be brought about by other types of defects such as dislocations which we will discuss in Sec. V B.

C. Lindemann criterion

We can compare our results with the Lindemann criterion by calculating the mean-square displacement $\langle |u|^2 \rangle$ at the transition using Eq. (5):

$$\langle |u|^2 \rangle = -\frac{2k_B T}{v_0} \sum_{\alpha k q} \frac{\partial \ln Z_{vib}}{\partial A(\alpha k q)}, \quad (23)$$

where A is given by Eq. (8) and α labels the two eigenvalues. Defining the Lindemann ratio c_L by $c_L^2 = \langle |u|^2 \rangle / a_0^2$, we find that $c_L \approx 0.25$ for YBCO at $H_m = 5$ T and that $c_L \approx 0.11$ for BSCCO at $H_m = 200$ G. Here we have used the same values of the parameters that were used to fit the phase transition curves in Fig. 2. These values of c_L are consistent with previous values.^{3,4,19}

D. Hysteresis

Experiments have found little, if any, hysteresis.^{5,12,14} This is consistent with our calculations. We can bound the hysteresis by noting the range of temperatures between which the liquid minimum appears and the solid minimum disappears. Typical values for the width of this temperature range are 300 mK for YBCO at $H = 5$ T and 1.3 K for BSCCO at $H = 200$ G. Another measure of the hysteresis can be found in the plots of Δf versus n (see inset of Fig. 2). The barrier height V_B between the minima is low ($V_B v_0 \sim 30$ mK) which is consistent with minimal hysteresis.

E. Loss of superconducting phase coherence

In going from the normal metallic phase to the vortex solid, two symmetries are broken: translational invariance and gauge symmetry which produces the superconducting phase coherence along the magnetic field. In the liquid, longitudinal superconductivity is destroyed by the wandering and entanglement of the vortex lines. Even though line wandering is energetically costly and therefore rare, it does occur. As a result, the correlation length along the c axis will be quite long and of order l_z . This is consistent with measurements in YBCO of the c -axis resistivity which find that there is loss of vortex velocity correlations for samples thicker than $100 \mu\text{m}$.^{69–71} For an infinitely thick sample, the loss of longitudinal superconductivity coincides with the melting transition.⁷² This agrees with experiments which indicate that the loss of superconducting phase coherence along the c axis coincides with the first-order transition.^{69–71}

IV. SURFACE TENSION

The vortex line wandering renormalizes the coupling between the planes in the liquid phase, so it is difficult to estimate the surface tension parallel to the ab planes which is primarily due to Josephson vortices. However, since we have expressions for the free energy in both the liquid and solid phases, we can estimate the surface tension parallel to the c axis along the melting curve. We imagine a plane interface parallel to the c axis between the vortex liquid and the vortex lattice phases. The surface tension σ is given by

$$\sigma = \int_{-\infty}^{\infty} [G(x) - G_0] dx, \quad (24)$$

where $G(x)$ is the Gibbs free energy as a function of position and the constant G_0 is the Gibbs free energy far away from the interface, for example within the solid phase where $n = 0$. (At melting the vortex liquid and solid phases coexist

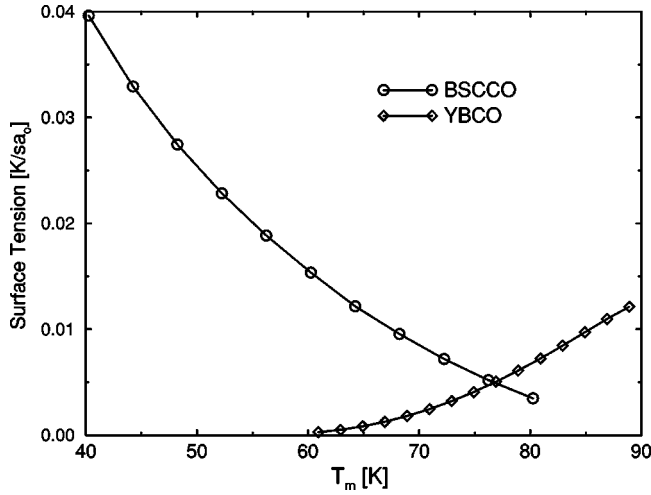


FIG. 4. Surface tension between the vortex solid and liquid phases along an interface parallel to the c axis versus melting temperature T_m . We use the values of field and temperature along the melting curve for YBCO and BSCCO. The surface tension is measured in units of Kelvin/ sa_0 , where s is the spacing between layers and $a_0 = \sqrt{\phi_0/B}$ is the vortex lattice spacing. The values of the parameters are the same as in Fig. 1.

because they have the same bulk value for the Gibbs free energy). In the interface region the defect concentration n changes from zero in the solid phase to a finite value in the liquid phase. Let us assume that in this region the concentration gradient dn/dx is a constant n_0/a_0 where n_0 is the concentration of defects in the bulk liquid phase. Here we are assuming that the width of the interface is of order a vortex lattice constant a_0 . Then

$$\sigma = \frac{a_0}{n_0} \int_0^{n_0} [G(n) - G_0] dn. \quad (25)$$

This is an integral of the area under the barrier between the solid and liquid phases in the plot of the Gibbs free energy versus defect concentration (see inset of Fig. 2). Using the values for T and B along the melting curve, we find the surface tension given in Fig. 4. The dependence of the surface tension on the melting temperature T_m reflects that of the barrier height V_B on T_m . The order of magnitude of the surface tension is given by $\sigma \sim V_B/sa_0$, and as a result, the values are quite small. For example, at $T = 60.24$ K and $B = 202.28$ G, $\sigma = 0.015$ K/ sa_0 for BSCCO, and at $T = 80.9184$ K and $H = 6.4807$ T, $\sigma = 7.26 \times 10^{-3}$ K/ sa_0 for YBCO, where s is the interplane spacing and $a_0 = \sqrt{\phi_0/B}$. We believe these are correct order of magnitude estimates for the surface tension since the small values of the barrier height is consistent with the small amount of hysteresis found experimentally.^{5,12,14}

V. VORTEX LIQUID

A. Viscoelastic behavior

We now discuss the viscoelastic behavior of the vortex liquid. As we mentioned earlier, the shear modulus is frequency dependent. The low-frequency response to a shear stress is the flow of vortices and this is characterized by a viscosity η . At high frequencies the response is elastic and

the crossover between the two occurs over a narrow frequency range so that the shear modulus as a function of frequency is rather like a step function. This behavior can be simply modeled using the Maxwell model⁷³ for viscoelasticity in which a massless spring is damped by a viscous force. The rate of shear strain $\dot{\epsilon}$ is given by

$$\dot{\epsilon} = \frac{\dot{\sigma}}{c_{66}(\omega = \infty)} + \frac{\sigma}{\eta}, \quad (26)$$

where σ is the shear stress, $\dot{\sigma}$ is the time derivative of the shear stress, and ω is the frequency. Using the Maxwell relation for the relaxation time $\tau = \eta/c_{66}(\omega = \infty)$ and the definition of the frequency dependent shear modulus $c_{66}(\omega) = \sigma(\omega)/\epsilon(\omega)$, we find that the real part of the shear modulus is given by

$$c_{66}(\omega) = c_{66}(\omega = \infty) \left[\frac{\omega^2 \tau^2}{1 + \omega^2 \tau^2} \right]. \quad (27)$$

Notice that $c_{66}(\omega = 0) = 0$ which confirms that the vortex liquid cannot sustain a shear stress. At high frequencies $c_{66}(\omega)$ is given by $c_{66}(\omega = \infty)$. To estimate the crossover frequency we need to estimate the viscosity.

We are interested in the shear viscosity which arises from the interactions between vortices. There are other sources of viscosity. For example a single moving vortex line experiences a viscous drag due to the normal electrons in the core which produce resistance when they move with the vortex. This is described by the Bardeen-Stephen model.⁴¹ There is also viscosity which arises from pinning; we will ignore this contribution since we are considering a clean lattice. We can obtain a simple estimate for the viscosity following the approach of Dyre, Olsen, and Christensen.⁷⁴ Shear flow occurs when some vortices push past other vortices. The viscosity η is given by

$$\eta = \eta_0 \exp \left[\frac{\Delta F(T)}{k_B T} \right], \quad (28)$$

where the prefactor η_0 is the viscosity of a single noninteracting vortex line and is given by the Bardeen-Stephen relation⁴¹ $\eta_0 \approx \phi_0 H_{c2} / \rho_n c^2$ where ρ_n is the normal-state resistivity and c is the speed of light. In Eq. (28) $\Delta F(T)$ is the activation energy which is identified with the work done per vortex pancake in shoving aside the surrounding vortices. The elastic energy associated with distorting the vortices is given by Eq. (6); we identify $\Delta F(T)$ with \mathcal{F}_{el} at the maximum distortion \mathbf{u} produced by the shoving. The actual form of the distortion is difficult to determine analytically. We will assume that the dominant contribution comes from tilt and shear; and that there is no change in the density so that the contribution from the bulk modulus can be ignored. In BSCCO in the vortex liquid, the planes are decoupled and the tilt modulus can be ignored. In YBCO in the liquid the correlation along the c axis can be quite long as we discussed earlier. In this case the distortion involves various wave vectors; the wave-vector dependence of the tilt modulus c_{44} is such that at small q , c_{44} is roughly comparable to the high-frequency shear modulus $c_{66}(\omega = \infty)$ and at large q , $c_{44} \ll c_{66}(\omega = \infty)$. (Since we are considering the elastic response,

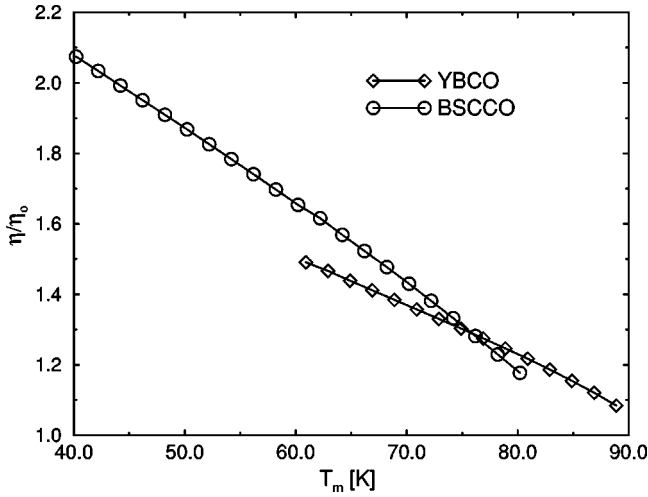


FIG. 5. Reduced viscosity η/η_0 of the vortex liquid versus melting temperature T_m along the melting curve for YBCO and BSCCO. $\delta=1$. The values of the parameters are the same as in Fig. 1.

it is appropriate to consider the high-frequency shear modulus.) So as a crude estimate we will assume the displacement is pure shear and write⁷⁵

$$\Delta F(T) = c_{66}(\omega = \infty, n, T) V_c, \quad (29)$$

where V_c is the volume change due to shoving and rearranging vortices. Since $\Delta F(T)$ is the energy per vortex pancake, V_c is some fraction δ of the volume v_0 per vortex pancake, i.e., $V_c = \delta v_0$. $c_{66}(\omega = \infty, n, T)$ is given by Eq. (18). In Fig. 5 we show the reduced viscosity η/η_0 along the melting line for both YBCO and BSCCO with $\delta=1$. As one can see, interactions enhance the viscosity η over the noninteracting viscosity η_0 by a factor of 2 or less. This is because $\Delta F(T_m)/k_B T_m < 1$ along the melting line.

Using our estimate of the viscosity and Eq. (27), we can calculate the frequency dependence of the shear modulus $c_{66}(\omega)$ as shown in Fig. 6 for a defect concentration of 5%. As expected the shear modulus has the shape of a step function; it is zero at low frequencies and rises quite sharply to its infinite frequency value $c_{66}(\omega = \infty)$. Notice that for BSCCO the crossover frequency is a few MHz and for YBCO it is a few GHz. Since 1 K corresponds to 20 GHz, this means that we made an excellent approximation in setting $c_{66} = c_{66}(\omega = \infty)$ in the free-energy density f in Eq. (1).

B. Dislocations

Any theory that tries to describe melting has to contain two main ingredients: a satisfactory description of both the solid and the liquid phases and a mechanism by which the system goes from one to the other. The difficulty has always been to describe two phases with wildly different properties within the same framework. In the present work, we have achieved this by viewing the liquid as a solid with a finite concentration of vacancies and interstitials. Clearly this is an approximation. If one wishes to describe a liquid as a solid with defects, other types of defects have to be taken into account as well. This is particularly true of dislocations. While it is unlikely that thermally excited dislocations play

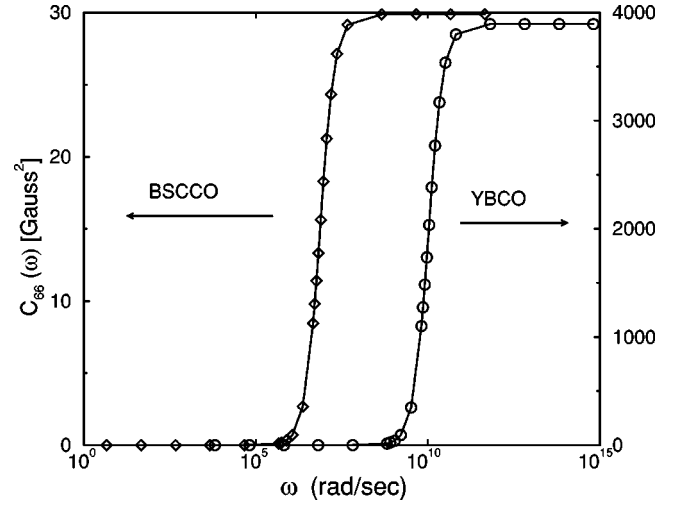


FIG. 6. Shear modulus c_{66} versus frequency for YBCO and BSCCO. For YBCO, $H=5$ T, $T=83$ K, and the defect concentration $n=4\%$. For BSCCO, $B=200$ G, $T=60$ K, and $n=5\%$. The values chosen are close to those on the melting curve. The rest of the values of the parameters are the same as in Fig. 1.

the key role in mediating the melting transition because of their high-energy cost, we think that they will proliferate as soon as the vacancies and interstitials appear. This proliferation of dislocations precludes the appearance of neutron-scattering Bragg peaks which would be expected if the liquid were just a lattice with a few percent of defect lines. While neutron scattering has detected Bragg peaks at one point above the melting curve of BSCCO,^{76,77} the structure of the liquid has not been determined via neutron scattering or muon spin resonance, e.g., neutron-scattering diffraction rings have not been observed in the vortex liquid.

There are two reasons to expect dislocations to proliferate. First interstitial vortex lines are usually attractive⁴⁷ and can aggregate to form dislocations that extend the entire length of the lattice parallel to the c axis. The same is true for vacancies. In particular, Olive and Brandt⁴⁷ have done numerical simulations on line defects which were at least five lattice spacings apart. They found that both centered and edge interstitials⁷⁵ are attractive if $\lambda_{ab}/a_0 \geq 1$. For $\lambda_{ab}/a_0 = 0.25$, edge interstitials were attractive for separations less than ten lattice spacings and repulsive at larger distances while centered interstitials were repulsive at distances larger than five lattice spacings. Vacancies were attractive in all cases.

The second reason is that the substantial softening of the shear modulus brought about by the vacancies and interstitials reduces the dislocation core energy as well as the elastic energy of creating dislocations. For example, the core energy of a z -directed dislocation goes as $c_{66}b^2$ and the core energy of a screw dislocation goes as $\sqrt{c_{66}c_{44}}b^2$ where b is the magnitude of the Burger's vector.³⁹ In addition the long-range interaction between dislocation loops is mediated by the strain field and depends on c_{66} .³⁹ Once the dislocations have proliferated, the method and results of Marchetti and Radzihovsky³⁹ can be used to provide a more detailed and accurate description of the liquid side of the transition. For example, they show that when dislocations at all length

scales are present, the shear modulus vanishes in the long-wavelength limit.^{38,39} Work in this direction is in progress.

VI. SUMMARY

To summarize, we have presented a model for the melting of a vortex lattice into a vortex liquid. The melting transition is induced by a few percent of vacancy and interstitial vortex lines that soften the shear modulus and increase the vibrational entropy. The increased vibrational entropy leads to melting. We obtain good agreement with the experimentally measured curve of transition temperature versus field, latent heat, and jumps in magnetization for BSCCO and YBCO. The Lindemann ratio c_L is $\sim 11\%$ for BSCCO and $\sim 25\%$

for YBCO. The hysteresis is small. We find a very small surface tension between the vortex solid and the vortex liquid along an interface parallel to the c axis. The shear modulus is frequency dependent; it is zero at $\omega=0$ and plateaus at higher frequencies to its infinite frequency value.

ACKNOWLEDGMENTS

We thank Andy Granato and Lev Bulaevskii for helpful discussions. This work was supported in part by ONR Grant No. N00014-96-1-0905 and by funds provided by the University of California for the conduct of discretionary research by Los Alamos National Laboratory.

-
- ¹D.R. Nelson, Phys. Rev. Lett. **60**, 1973 (1988).
²D.S. Fisher, M.P.A. Fisher, and D.A. Huse, Phys. Rev. B **43**, 130 (1991).
³G. Blatter *et al.*, Rev. Mod. Phys. **66**, 1125 (1994).
⁴E.H. Brandt, Rep. Prog. Phys. **58**, 1465 (1995).
⁵H. Safar *et al.*, Phys. Rev. Lett. **70**, 3800 (1993).
⁶R. Liang, D.A. Bonn, and W.N. Hardy, Phys. Rev. Lett. **76**, 835 (1996).
⁷U. Welp *et al.*, Phys. Rev. Lett. **76**, 4809 (1996).
⁸A. Schilling *et al.*, Nature (London) **382**, 791 (1996).
⁹A. Schilling *et al.*, Phys. Rev. Lett. **78**, 4833 (1997).
¹⁰A. Schilling *et al.*, Phys. Rev. B **58**, 11 157 (1998).
¹¹M. Roulin, A. Junod, A. Erb, and E. Walker, Phys. Rev. Lett. **80**, 1722 (1998).
¹²E. Zeldov *et al.*, Nature (London) **375**, 373 (1995).
¹³D.T. Fuchs *et al.*, Phys. Rev. B **54**, R796 (1996).
¹⁴C.D. Keener *et al.*, Phys. Rev. Lett. **78**, 1118 (1997).
¹⁵T. Sasagawa *et al.*, Phys. Rev. Lett. **80**, 4297 (1998).
¹⁶A. Schilling *et al.*, Physica C **282-287**, 327 (1997).
¹⁷H. Pastoriza, M.F. Goffman, A. Arribère, and F. de la Cruz, Phys. Rev. Lett. **72**, 2951 (1994).
¹⁸E. Breézin, D.R. Nelson, and A. Thiaville, Phys. Rev. B **31**, 7124 (1985).
¹⁹A. Houghton, R.A. Pelcovits, and A. Sudbó, Phys. Rev. B **40**, 6763 (1989).
²⁰R.E. Hetzel, A. Sudbó, and D.A. Huse, Phys. Rev. Lett. **69**, 518 (1992).
²¹R. Šašik and D. Stroud, Phys. Rev. Lett. **75**, 2582 (1995).
²²S. Ryu and D. Stroud, Phys. Rev. B **54**, 1320 (1996).
²³S. Ryu and D. Stroud, Phys. Rev. Lett. **78**, 4629 (1997).
²⁴X. Hu, S. Miyashita, and M. Tachiki, Phys. Rev. Lett. **79**, 3498 (1997).
²⁵X. Hu, S. Miyashita, and M. Tachiki, Phys. Rev. B **58**, 3438 (1998).
²⁶A.K. Nguyen, A. Sudbó, and R.E. Hetzel, Phys. Rev. Lett. **77**, 1592 (1996).
²⁷A.K. Nguyen and A. Sudbó, Phys. Rev. B **57**, 3123 (1998).
²⁸H. Nordborg and G. Blatter, Phys. Rev. Lett. **79**, 1925 (1997).
²⁹D.R. Nelson and H.S. Seung, Phys. Rev. B **39**, 9153 (1989).
³⁰Y.-H. Li and S. Teitel, Phys. Rev. B **49**, 4136 (1994).
³¹Z. Tešanović, Phys. Rev. B **51**, 16 204 (1995).
³²J. Kierfeld and V. Vinokur, cond-mat/9909190 (unpublished).
³³A.V. Granato, Phys. Rev. Lett. **68**, 974 (1992).
³⁴H.M. Carruzo and C.C. Yu, Philos. Mag. B **77**, 1001 (1998).
³⁵F. P. Preparata and M. I. Shamos, *Computational Geometry* (Springer-Verlag, New York, 1985).
³⁶P. Kim, Z. Yao, and C.M. Lieber, Phys. Rev. Lett. **77**, 5118 (1996).
³⁷E. Frey, D.R. Nelson, and D.S. Fisher, Phys. Rev. B **49**, 9723 (1994).
³⁸M.C. Marchetti and D.R. Nelson, Phys. Rev. B **41**, 1910 (1990).
³⁹M.C. Marchetti and L. Radzihovsky, Phys. Rev. B **59**, 12 001 (1999).
⁴⁰To estimate $\epsilon_0 s$ for YBCO, we used $s=12 \text{ \AA}$ and $\lambda_{ab}(T) = \lambda_{ab}(0)[1 - (T/T_c)]^{-1/3}$ with $\lambda_{ab}(0)=1186 \text{ \AA}$ (Ref. 46) and $T_c=93 \text{ K}$. For BSCCO we used $s=14 \text{ \AA}$ and $\lambda_{ab}^2(T) = \lambda_{ab}^2(0)/[1 - (T/T_c)^4]$ (Ref. 41) with $\lambda_{ab}(0)=2000 \text{ \AA}$ and $T_c=90 \text{ K}$.
⁴¹M. Tinkham, *Introduction to Superconductivity*, 2nd ed. (McGraw-Hill, New York, 1996).
⁴²P. G. de Gennes, *Superconductivity of Metals and Alloys* (Addison-Wesley, Redwood City, 1989).
⁴³L.N. Bulaevskii, M. Ledvij, and V.G. Kogan, Phys. Rev. Lett. **68**, 3773 (1992).
⁴⁴E.H. Brandt, J. Low Temp. Phys. **26**, 735 (1977).
⁴⁵E.H. Brandt, J. Low Temp. Phys. **26**, 709 (1977).
⁴⁶S. Kamal *et al.*, Phys. Rev. Lett. **73**, 1845 (1994).
⁴⁷E. Olive and E.H. Brandt, Phys. Rev. B **57**, 13 861 (1998).
⁴⁸E.H. Brandt, Phys. Rev. B **56**, 9071 (1997).
⁴⁹A.V. Granato, J. Phys. Chem. Solids **55**, 931 (1994).
⁵⁰J.T. Holder, A.V. Granato, and L.E. Rehn, Phys. Rev. Lett. **32**, 1054 (1974).
⁵¹J.T. Holder, A.V. Granato, and L.E. Rehn, Phys. Rev. B **10**, 363 (1974).
⁵²L.E. Rehn *et al.*, Phys. Rev. B **10**, 349 (1974).
⁵³P.H. Dederichs *et al.*, J. Nucl. Mater. **69**, 176 (1978).
⁵⁴Although calculations indicate that fluctuations in the density of vacancies and interstitial defects do not renormalize c_{66} (Ref. 39), c_{66} does decrease as the average number of defects increases.
⁵⁵H. Pastoriza and P.H. Kes, Phys. Rev. Lett. **75**, 3525 (1995).
⁵⁶H. Won and K. Maki, Phys. Rev. B **53**, 5927 (1996).
⁵⁷M. Yethiraj *et al.*, Phys. Rev. Lett. **70**, 857 (1993).
⁵⁸B. Keimer *et al.*, Phys. Rev. Lett. **73**, 3459 (1994).
⁵⁹I. Maggio-Aprile *et al.*, Phys. Rev. Lett. **75**, 2754 (1995).
⁶⁰Our ϕ equals half the angle cited in the experiments.

- ⁶¹L.I. Glazman and A.E. Koshelev, Phys. Rev. B **43**, 2835 (1991).
- ⁶²L.L. Daemen, L.N. Bulaevskii, M.P. Maley, and J.Y. Coulter, Phys. Rev. Lett. **70**, 1167 (1993).
- ⁶³G. Blatter, V. Geshkenbein, A. Larkin, and H. Nordborg, Phys. Rev. B **54**, 72 (1996).
- ⁶⁴B. Horovitz and T.R. Goldin, Phys. Rev. Lett. **80**, 1734 (1998).
- ⁶⁵M.J.W. Dodgson, V.B. Geshkenbein, and G. Blatter, cond-mat/9902244 (unpublished).
- ⁶⁶M.J.W. Dodgson, V.B. Geshkenbein, H. Nordborg, and G. Blatter, Phys. Rev. Lett. **80**, 837 (1998).
- ⁶⁷M.J.W. Dodgson, V.B. Geshkenbein, H. Nordborg, and G. Blatter, Phys. Rev. B **57**, 14 498 (1998).
- ⁶⁸A.I.M. Rae, E.M. Forgan, and R.A. Doyle, Physica C **301**, 301 (1998).
- ⁶⁹D. Lopez, E.F. Righi, G. Nieva, and F. de la Cruz, Phys. Rev. Lett. **76**, 4034 (1996).
- ⁷⁰D. Lopez *et al.*, Phys. Rev. B **53**, R8895 (1996).
- ⁷¹D. Lopez (private communication).
- ⁷²T. Chen and S. Teitel, Phys. Rev. Lett. **74**, 2792 (1995).
- ⁷³J.-P. Hansen and I. R. McDonald, *Theory of Simple Liquids*, 2nd ed. (Academic Press, London, 1986), p. 293, for example.
- ⁷⁴J.C. Dyre, N.B. Olsen, and T. Christensen, Phys. Rev. B **53**, 2171 (1996).
- ⁷⁵Another way to estimate the free energy $\Delta F(T)$ in Eq. (28) is to use the energy difference between a centered interstitial and an edge interstitial (Refs. 37 and 47). A centered interstitial vortex line is at the center of a triangle whose vertices are the nearest-neighbor lattice sites of a triangular lattice. An edge interstitial lies at the midpoint of one of the sides of the triangle. Numerical calculations (Refs. 37 and 47) find this energy to be roughly $10^{-3} \times 2 \epsilon_0 \sim 1 \text{ K} \ll T_m$. So on the melting curve, $\eta/\eta_0 \approx 1$. This estimate of $\Delta F(T)$ is an order of magnitude smaller than the estimate we used in Eq. (29). As a result the crossover frequency, where $c_{66}(\omega)$ goes from its low-frequency to its high-frequency value, increases by less than a factor of 2 compared to the crossover frequencies shown in Fig. 6.
- ⁷⁶E.M. Forgan *et al.*, Czech. J. Phys. **46**, 1571 (1996).
- ⁷⁷D.T. Fuchs *et al.*, Phys. Rev. Lett. **80**, 4971 (1998).